

## VISCOSITY EFFECTS ON STEADY IRREGULAR REFLECTION OF SHOCK WAVES

Dmitry Khotyanovsky, Yevgeniy Bondar, Alexey Kudryavtsev,  
Georgy Shoev, and Mikhail Ivanov

*Computational Aerodynamics Lab  
Khristianovich Institute of Theoretical and Applied Mechanics  
Siberian Branch of the Russian Academy of Sciences  
Institutskaya 4/1, Novosibirsk 630090, Russia*

**Key words:** weak shock reflection, von Neumann paradox, steady flow.

**Abstract.** The effects of flow viscosity on weak shock wave reflection are investigated with the Navier–Stokes and DSMC flow solvers. It is shown that the viscosity plays crucial role in the vicinity of three-shock intersection at the parameters corresponding to the von Neumann reflection of shock waves in steady flow. Instead of a singular triple point, in viscous flow there is a smooth shock transition zone, where one-dimensional shock jump relations cannot be applied.

### 1. BACKGROUND AND MOTIVATION

Many interesting phenomena that occur in oblique shock wave reflection have been discovered in the past. Main feature herein is the existence of two possible configurations of shocks, regular and irregular. Regular reflection consists of the incident shock wave and the reflected shock wave with supersonic flow behind the reflected shock. Irregular reflection, which is in most cases called Mach reflection due to E. Mach who first discovered this phenomenon, is a complex shock wave pattern that combines the incident, reflected shock waves and the Mach stem. A contact discontinuity (slipstream) emanates from the triple point due to inequality of entropy in the flow passing through the incident and reflected shocks and the flow passing through the Mach stem. Classical theoretical methods such as shock polar analysis and the three-shock theory based on Rankine–Hugoniot jump conditions across the oblique shocks were developed by J. von Neumann to describe the shock wave configurations at various flow parameters and to predict transitions between different types of shock wave interaction. These theoretical methods predict well most of the features of shock wave interaction.

Steady shock wave reflection is very important in aerodynamics and has been extensively studied in recent years with emphasis to strong shock waves (for flow Mach number higher than 2.2 in air). However, for supersonic civil aviation the lower Mach number range is most interesting. Regular and irregular interactions of different types are inherent in such critical phenomena as off-design inlet flows, inlet starting and flow stalling. Interactions and reflections of weak shock waves are typical for supersonic inlet flows at low and moderate Mach numbers ( $M=1-2$ ).

There are many problems of irregular shock reflections in steady flows which are not yet investigated. One of the most exciting phenomena that occurs in irregular reflection of weak shock waves is a shock wave reflection in the range of flow parameters where the von Neumann's three-shock theory does not produce any solution whereas the experiments reveal [1] a three-shock structure similar to the Mach reflection pattern. This inconsistency is referred to as the von Neumann paradox, and the observed reflection pattern as the von Neumann reflection (vNR). Inviscid numerical simulations of the pseudo-steady shock wave reflection at the conditions of the von Neumann paradox conducted in [1] with a second-order Godunov-type scheme showed that the incident and Mach shocks "appear to form a single wave with a continuously turning tangent". The Euler computations performed later in [2] with a specifically-designed shock-fitting algorithm argued that the grid resolution in the vicinity of the triple point is essential in this problem and found many interesting flow details.

Many efforts were made to develop a consistent inviscid theory of the vNR. Those studies were mainly concerned with the pseudo-steady reflection of a shock wave running over a wedge. As soon as the three-shock solution does not exist at the von Neumann paradox conditions, some additional gasdynamic features are introduced to solve the problem (local supersonic patch, compression wave, etc.). In the second group of works, the vNR is explained by the effects of flow viscosity ([3]). Due to finite thickness of the interacting shock waves the flow in the vicinity of the triple point is substantially different from the inviscid flow. As stated in [3], at the intersection there must be a zone of essentially two-dimensional flow, which he labels "non Rankine-Hugoniot shock wave zone", where the gradients of flow parameters in the direction tangent to the shock wave are important. This non-R-H zone acts as a buffer zone separating R-H shocks in the upper and lower domains. The size of this non-R-H zone was estimated as a few shock wave thicknesses. It is therefore impossible to confirm or reject the existence of such a viscous zone via inspection of the experimental data because of the insufficient resolution of the flow field in the experiment. We believe that the numerical computations can help clarify this.

## 2. PROBLEM FORMULATION AND NUMERICAL TECHNIQUES

In this study we investigate irregular reflection of weak shock waves in steady supersonic flow with Mach number  $M_\infty$  between two symmetrical wedges with equal angles of attack  $\theta_w$ . The shock wave reflection occurs at the plane of symmetry half-way between the wedges. Necessary length scale is introduced in this problem due to influence of the expansion waves emanating from the trailing edges of the wedges. The wedge chord,  $w$ , was chosen as the length scale. The flow geometry is controlled with the parameter  $g/w$ , which is the ratio of the distance between the trailing edges  $g$  to the wedge chord  $w$ .

Characteristic feature of the weak shock wave reflection is that the flow behind the reflected shock wave of the Mach reflection is subsonic. For a gas with specific heats ratio  $\gamma$  there is a Mach number value  $M_c$ , at which the shock wave angles corresponding to the detachment  $\alpha_d$  and the von Neumann  $\alpha_N$  conditions coincide:  $M_c \approx 2.2$  for diatomic gases with  $\gamma = 1.4$ , and  $M_c \approx 2.47$  for monatomic gases with  $\gamma = 5/3$ . At flow Mach number  $M_\infty < M_c$  the reflected shock wave of the MR belongs to the strong family, and hence the flow behind the reflected shock is subsonic.

It is convenient to illustrate various conditions on pressure-deflection diagrams, see Fig. 1, where different shock polar combinations for  $\gamma = 5/3$  and  $M_\infty = 1.7$

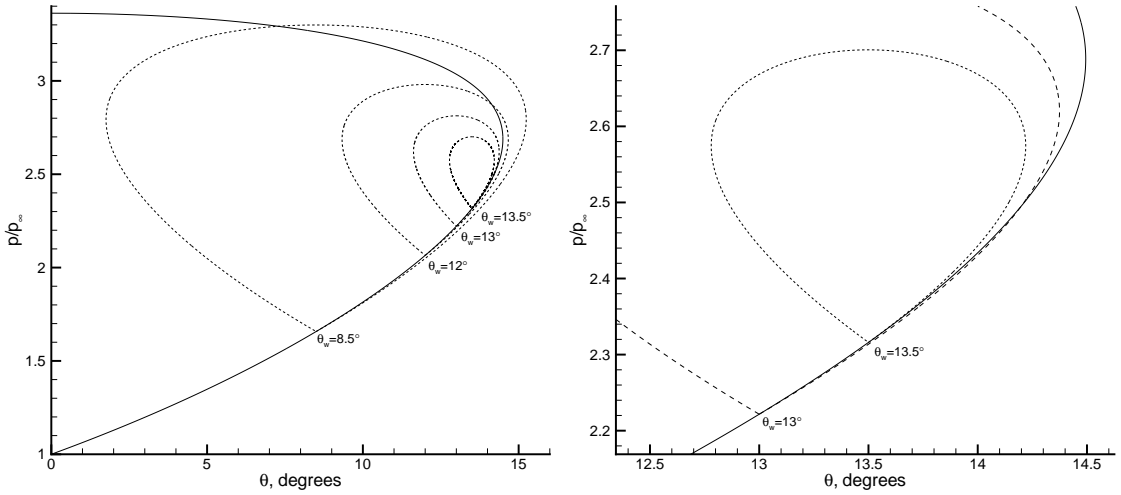


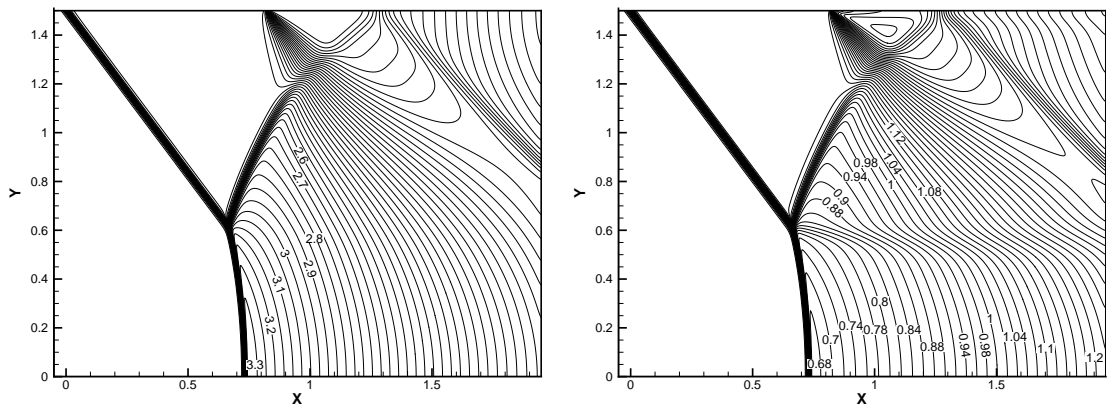
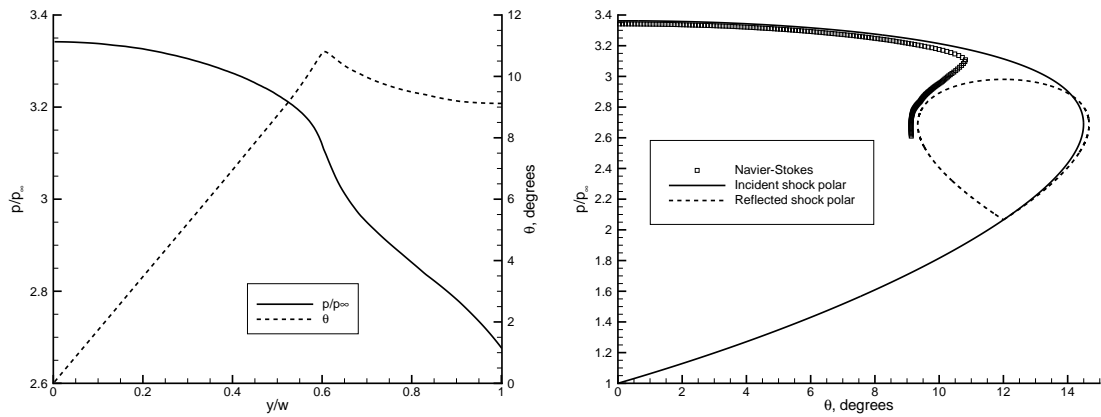
Figure 1: Pressure-deflection diagrams for  $\gamma = 5/3$ ,  $M_\infty = 1.7$ . Incident shock polar is solid, reflected shock polars for various wedge angles  $\theta_w$  are dashed

are given. The intersection of the reflected shock polar with the incident shock polar indicates matching pressure  $p_{ss}$  and flow deflection at the slipstream  $\theta_{ss}$ , and represents a three-shock solution. These solutions are listed in Table for various  $\theta_w$ . For reference, Mach number behind the reflected shock  $M_{rs}$  is also given in the last column of Table. At  $\theta_w = 8.5^\circ$  the shock polar intersection yields a three-shock solution corresponding to an MR with subsonic flow behind the reflected shock wave. The deflection angle of the flow passing through the reflected shock is decreased. At  $\theta_w = 9.627^\circ$  the reflected shock wave becomes normal to the flow, and the flow deflection is not changed. At higher angles, the reflected shock wave predicted by the three-shock solution is inclined forward with respect to the flow, and the flow deflection in the reflected shock is increased. The three-shock solution obtained at  $\theta_w = 13^\circ$  predicts a forward-inclined reflected shock wave with supersonic flow behind it. Such a configuration cannot exist, and the solution should be discarded.  $\theta_w = 13.5^\circ$  does not produce any three-shock solution since the reflected shock polar does not intersect the incident shock polar. This latter case corresponds to the von Neumann paradox conditions.

In this study we investigate numerically some of these shock wave reflection configurations. The computations are conducted with both Navier–Stokes equations and the DSMC (Direct Simulation Monte Carlo) method. The computations are performed at low Reynolds number of the flow with full resolution of the internal structure of the shock waves. The Navier–Stokes code is a time-explicit shock capturing code based on WENO-5 [4] discretization of the convective terms, and the central-difference discretization of the diffusive terms. The DSMC simulations are performed with the SMILE code [5]. The grid resolution studies were made to ensure that the shock wave profiles are properly resolved.

To eliminate possible non-equilibrium effects a monatomic gas, Argon, with  $\gamma = 5/3$  is considered. Power-law dependence of the viscosity coefficient on temperature with exponent 0.81 is used in the Navier–Stokes. The computations were performed at flow Mach number  $M_\infty = 1.7$ . Reynolds number was typically  $Re = 1000$ .

$\theta_w$	$p_{ss}/p_\infty$	$\theta_{ss}$	$M_{rs}$
8.5	3.293	7.275	0.7780
9.627	3.227	9.627	0.7999
12	2.873	14.13	0.9008
13	2.495	14.20	1.011

 Table 1: Three-shock solutions at  $\gamma = 5/3$ ,  $M_\infty = 1.7$  at various wedge angles  $\theta_w$ 

 Figure 2: Pressure contours (left) and Mach number contours (right). Navier-Stokes computations at  $\gamma = 5/3$ ,  $M_\infty = 1.7$ ,  $Re = 1000$ ,  $\theta_w = 12^\circ$ 

 Figure 3: Pressure and flow deflection variation along the Mach stem and reflected shock. Navier-Stokes computations at  $\gamma = 5/3$ ,  $M_\infty = 1.7$ ,  $Re = 1000$ ,  $\theta_w = 12^\circ$

### 3. RESULTS AND DISCUSSIONS

The results of the Navier–Stokes computations at  $\theta_w = 12^\circ$  are illustrated in Fig. 2. The obtained shock wave reflection resembles a typical MR pattern, though smeared by the flow viscosity. Instead of the triple point we have a smooth continuous transition from the Mach stem to the reflected shock, which we label the triple-shock zone. Closed subsonic region is formed behind the Mach stem and the reflected shock. The size of this region is governed by the geometry parameter  $g/w$ , which is  $g/w = 1.5$  in this case. The flow portions passing through the Mach stem and the reflected shock are separated with the mixing layer. The reflected shock wave is curved due to the influence of expansion waves that cause pressure drop in the subsonic flow behind the reflected shock. An interesting observation that can be made inspecting the pressure distribution is that the pressure rise in the reflected shock wave is followed by gradual pressure increase downstream of the reflected shock. This also concerns the part of the flow just behind the triple-shock zone. This pressure rise can be explained by the influence of the disturbances from high-pressure flow behind the Mach stem that reach the flow behind the reflected shock through the subsonic region.

In Fig. 3 the distributions of pressure and flow deflection along the curve passing just behind the Mach and reflected shock are given. The pressure monotonously decreases when moving upwards along the Mach stem and the reflected shock. There is an apparent slope change in the pressure variation just behind the triple-shock zone at  $y/w \approx 0.65$ . The flow deflection increases when moving up behind the Mach stem, reaches its maximum behind the triple-shock region, and then decreases as the reflected shock becomes more and more curved. An interesting observation is that the flow deflection behind the triple-shock zone does not exceed the flow deflection behind the incident shock  $\theta_w = 12^\circ$ . This contradicts the three-shock solution, which predicts  $\theta = 14.13^\circ$  at the slipstream given in Table . This is most evident in the right plot of Fig. 3, where we compared our numerical results with shock polars in the  $(p, \theta)$  plane. The pressures and flow deflection are really close to shock polars far from the triple-shock region, and deviate from the shock-polar solutions in the vicinity of the shock intersection where the viscosity effects are strong. Note, that the deviation of the flow parameters from the shock polars effectively means that Rankine–Hugoniot relations are not valid within the viscous triple-shock zone.

The results of the Navier–Stokes computations at  $\theta_w = 13.5^\circ$ , i.e. at the von Neumann paradox conditions, are presented in Figs. 4 and 5. Although there is no three-shock solution in this case, the Navier–Stokes computations clearly demonstrate a triple-shock pattern similar to those observed in the previous case. The reflected shock wave is much weaker in this case, since the flow Mach number behind the incident shock is close to unity  $M = 1.064$ . The results of the DSMC computations performed at the von Neumann paradox conditions ( $\gamma = 7/5$ ,  $M_\infty = 1.5$ ,  $\theta_w = 10^\circ$ ) (see Fig. 6) are in good qualitative agreement with the Navier–Stokes computations.

Our simulations performed with substantially different approaches suggest that the flow viscosity causes formation of a smooth shock transition zone in the triple-shock region, where one-dimensional shock jump relations cannot be applied.

**Acknowledgments.** This study was supported by the Russian Foundation for Basic Research (Grant 06-01-22000) and the Fundamental Research Program 14 of the Russian Academy of Sciences. The computations were performed at the Siberian Supercomputer Centre, Novosibirsk and the Joint Supercomputer Centre, Moscow.

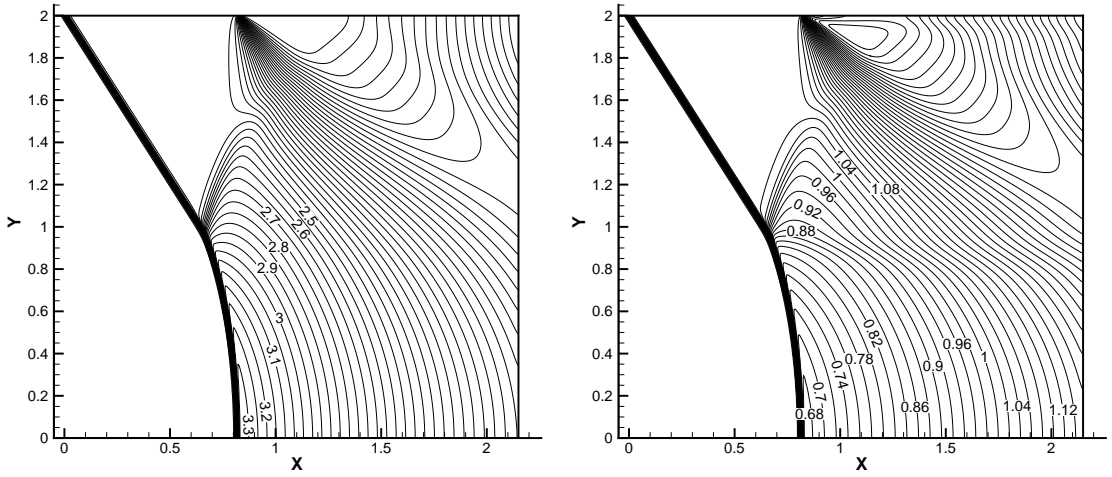


Figure 4: Pressure contours (left) and Mach number contours (right). Navier-Stokes computations at the von Neumann paradox conditions:  $\gamma = 5/3$ ,  $M_\infty = 1.7$ ,  $Re = 1000$ ,  $\theta_w = 13.5^\circ$

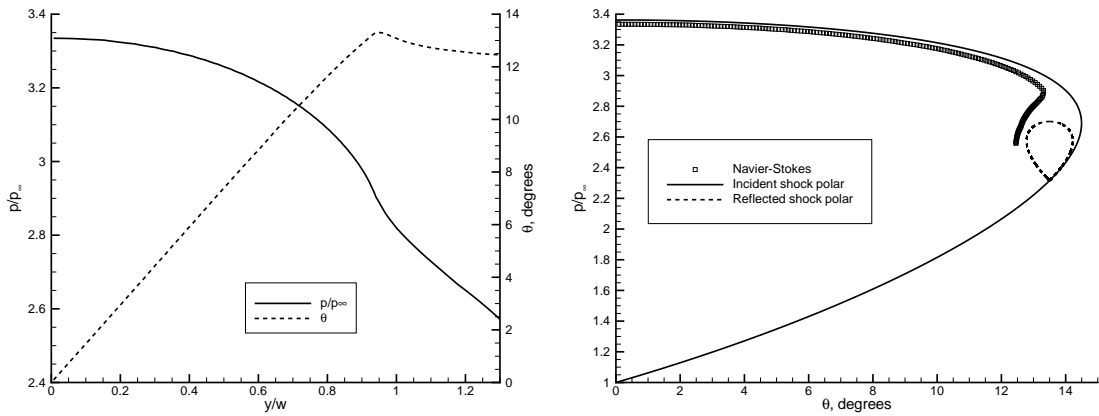


Figure 5: Pressure and flow deflection variation along the Mach stem and reflected shock. Navier-Stokes computations at  $\gamma = 5/3$ ,  $M_\infty = 1.7$ ,  $Re = 1000$ ,  $\theta_w = 13.5^\circ$

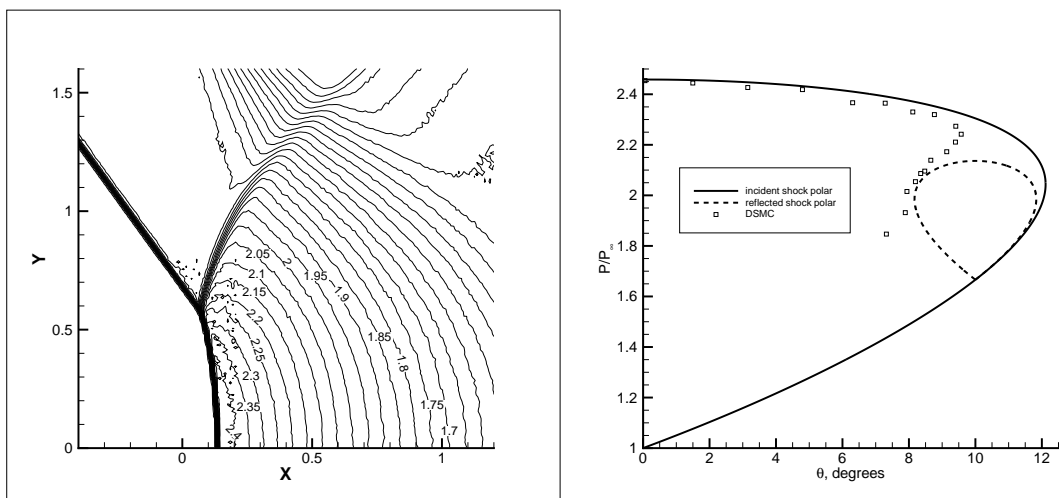


Figure 6: Pressure contours (left) and pressure-deflection variation (right) obtained in the DSMC computations at  $\gamma = 7/5$ ,  $M_\infty = 1.5$ ,  $Re_\infty = 1834$ ,  $\theta_w = 10^\circ$

## References

- [1] P. Colella, L.F. Henderson: J. Fluid Mech. **213** (1990)
- [2] E.I. Vasilyev, A.N. Kraiko: Computational Mathematics and Mathematical Physics **39(8)** (1999).
- [3] J. Sternberg: Phys. Fluids **2(2)** (1959)
- [4] G. Jiang, C.-W. Shu: J. Comput. Phys. **126** (1996).
- [5] M.S. Ivanov, G.N. Markelov, S.F. Gimelshein: AIAA Paper 98-2669, (1998).